A&A 540, A47 (2012)
DOI: 10.1051/0004-6361/201118660


Astronomy & Astrophysics

# The AMIGA sample of isolated galaxies

## X. A first look at isolated galaxy colors⋆

M. Fernández Lorenzo[1], J. Sulentic[1], L. Verdes-Montenegro[1], J. E. Ruiz[1], J. Sabater[2], and S. Sánchez[1]

Instituto de Astrofísica de Andalucía, Granada, IAA-CSIC Apdo. 3004, 18080 Granada, Spain
e-mail: mirian@iaa.es
Institute for Astronomy, University of Edinburgh, Edinburgh EH9 3HJ, UK

Received 16 December 2011 / Accepted 25 January 2012

**ABSTRACT**

*Context.* The basic properties of galaxies can be affected by both nature (internal processes) or nurture (interactions and effects of environment). Deconvolving the two effects is an important current effort in astrophysics. Observed properties of a sample of isolated galaxies should be mainly the result of internal (natural) evolution. It follows that nurture–induced galaxy evolution can only be understood through a comparative study of galaxies in different environments.
*Aims.* We take a first look at SDSS $(g - r)$ colors of galaxies in the AMIGA sample, which consists of many of the most isolated galaxies in the local Universe. This alerted us at the same time to the pitfalls of using automated SDSS colors.
*Methods.* We focused on median values for the principal morphological subtypes found in the AMIGA sample (E/S0 and Sb-Sc) and compared them with equivalent measures obtained for galaxies in denser environments.
*Results.* We find a weak tendency for AMIGA spiral galaxies to be redder than objects in close pairs. We find no clear difference when we compared this with galaxies in other (e.g. group) environments. However, the $(g - r)$ color of isolated galaxies shows a Gaussian distribution, as might be expected assuming nurture-free evolution. We find a smaller median absolute deviation in colors for isolated galaxies compared to both wide and close pairs. The majority of the deviation on median colors for spiral subtypes is caused by a color-luminosity correlation. Surprisingly, isolated and non-isolated early-type galaxies show similar $(g - r)$. We see little evidence for a green valley in our sample because most spirals redder than $(g - r) = 0.7$ have spurious colors.
*Conclusions.* The redder colors of AMIGA spirals and lower color dispersions for AMIGA subtypes – compared with close pairs – are likely caused by a more passive star formation in very isolated galaxies.

**Key words.** galaxies: evolution – galaxies: interactions – galaxies: fundamental parameters – galaxies: general

## 1. Introduction

In some ways our study of galaxy properties is still in its infancy. We have a plethora of theoretical ideas but we are still trying to understand what the basic measures such as size, luminosity, and color are telling us. This is partly because galaxies are composite structures and also because we cannot easily separate effects of nature (internal processes) from nurture (interactions and effects of environment).

The optical colors of galaxies reflect their stellar populations and these colors correlate with morphology and environment. The distribution of galaxy colors in the $(g - r)$ vs. $(u - g)$ plane (Strateva et al. 2001) shows a strong bimodality with clear separation into red and blue sequences. The study of morphology and spectral classification (Strateva et al. 2001) for subsamples of 287 red and 500 blue galaxies shows that the two color peaks correspond roughly to early – (E, S0, and Sa) and late-type (Sb, Sc, and Irr) galaxies, as expected from the respective dominance of old and young stellar populations. Colors of galaxies also strongly depend on luminosity in the sense that more luminous galaxies of the same morphological type are redder (Baldry et al. 2004). The color–magnitude relation is most obvious in the rest-frame $(g - r)$ (corrected to $z = 0.1$), where the separation between the red and blue populations is evident (Blanton et al. 2003).

Environment is also thought to play a role in the mix of morphological types for a sample of galaxies, which is reflected by the morphology-density relation (Dressler 1980; van der Wel et al. 2010, and references therein). In dense environments luminous red early-type galaxies predominate while in the lowest density environment blue late-type spirals are the defining population (Dressler 1980; Capak et al. 2007). While it is easy to recognize a rich cluster, definitions of low-density environments can be confusing. In recent years there has been an increased emphasis on identifying low density or isolated galaxy populations. One of the most useful samples remains the visually selected Catalog of Isolated Galaxies (CIG) compiled by Karachentseva (1973), more recently vetted as the AMIGA sample (Analysis of the interstellar Medium of Isolated GAlaxies, Sulentic 2010, and references therein).

Star formation is strongly dependent on the environment and shows an increased activity toward low-density environments (Lewis et al. 2002; Hogg et al. 2003, 2004; Baldry et al. 2006). In this sense, Balogh et al. (1998) found that the mean star formation rate in galaxies with similar bulge-to-total (B/T) luminosity ratios is always lower in clusters than in the field. However, Patton et al. (2011) found that the opposite is happening in galaxy pairs with clear signs of star formation induced by interaction within the blue galaxies. This result agrees with the bluer $(U - B$ and $B - V)$ colors found previously by Larson & Tinsley (1978) for peculiar galaxies.

⋆ Full Tables 1 and 2 are only available at the CDS via anonymous ftp to cdsarc.u-strasbg.fr (130.79.128.5) or via http://cdsarc.u-strasbg.fr/viz-bin/qcat?J/A+A/540/A47

Approximately 10% of the low-density universe is populated by pairs (also by triplets and dense groups) where environmental effects can reproduce the processes that happen in starburst galaxies and clusters (e.g. Xu & Sulentic 1991; Iovino 2002). This means that there are two sources of environmental effects: 1) the morphology-density relation and 2) one-on-one galaxy interactions, which can be found in a wide range of density environments. In this sense, the AMIGA vetting of the CIG (see below) is intended to produce an isolated sample that minimizes both effects.

The AMIGA project is producing and analyzing a multiwavelength database for a refinement of the CIG (Karachentseva 1973, $n = 1050$ galaxies). We have evaluated and improved the sample in different ways: 1) revision of all CIG positions in the sky (Leon & Verdes-Montenegro 2003); 2) optical characterization of the sample including completeness, luminosities, and heliocentric velocities (Verdes-Montenegro et al. 2005, and Sect. 2 of this paper); 3) morphological refinement and identification of galaxies with asymmetries (Sulentic et al. 2006, and Sect. 2.2 of this paper); and 4) quantification of the degree of isolation including the number density to the fifth neighbor ($\eta_k$) and estimation of the tidal force ($Q$) (Verley et al. 2007a,b).

The multiwavelength analysis of our AMIGA sample has shown that isolated galaxies have different properties from galaxies in higher density environments (even field samples). Variables expected to be enhanced by interactions are lower in AMIGA than any other sample, such as a lower infrared luminosity ($L_{FIR} < 10.5\ L_\odot$) and colder dust temperature (Lisenfeld et al. 2007), a low level of radio continuum emission dominated by mild disk star formation (Leon et al. 2008), no radio active galactic nuclei (AGN) selected using the radio-far infrared correlation (0%; Sabater et al. 2008) and a small number of optical AGN (22%; Sabater et al. 2012), a smaller fraction of asymmetric HI profiles (<20%, Espada et al. 2011), and less molecular gas (Lisenfeld et al. 2011). In addition, early-type galaxies in AMIGA are fainter than late types, and more AMIGA spirals host pseudo-bulges rather than classical bulges (Durbala et al. 2008). The data are being released and periodically updated at http://amiga.iaa.es, where a Virtual Observatory compliant web interface with different query modes has been implemented.

This paper presents a first look at colors for the AMIGA sample. It now becomes possible to analyze more than half of the AMIGA sample using uniform digital images, magnitudes, and colors of the Sloan digital sky survey (SDSS, York et al. 2000). In Sect. 2, the data revision of the AMIGA sample is provided. The sample selection is presented in Sect. 3, and the determination of the absolute magnitudes is described in Sect. 4. The dependence of the rest-frame color as a function of the morphological type and environment is analyzed in Sects. 5 and 6, respectively. Finally, the conclusions are presented in Sect. 7.

## 2. The AMIGA data revision

Because a significant number of new data are available for the sample since the project started, we have revised the apparent magnitudes, morphological types, distances, and optical luminosities for the CIG sample with respect to those used in Verdes-Montenegro et al. (2005) and Lisenfeld et al. (2007). In the frame of the Wf4Ever project[1], the revision of these properties was partially automated by the implementation of scientific workflows that ask for and gather values of some of the properties for all AMIGA galaxies from the HyperLeda catalog (see details below). These workflows also allow a comparison between values stored in the AMIGA database coming from different releases, registering the new values while keeping a version of the old ones. Therefore the methodology to calculate these values is stored in these workflows, which enables them to be reproduced and re-used, and even provides a re-purposability for similar cross-boundary use cases. Currently, releases of data in HyperLeda are not registered, hence while the methodology can be preserved, as explained above, traceability of the HyperLeda data is not possible yet. These workflows have been built in the Taverna Workflow Mamagement System[2] and can be accessed in the MyExperiment portal[3]. The data for the full AMIGA sample are listed in Table 1, and are also available in the AMIGA VO compliant interface. We describe the details of the revision below. For completeness, we explain here the entire revised parameters, although optical luminosity was not used in this paper.

### 2.1. Velocities and distances

We searched for new velocities for those CIG with heliocentric velocities ($V_{hel}$) higher than 1000 km s$^{-1}$, because for lower values redshift-independent distance estimates were preferred, and the same as in Verdes-Montenegro et al. (2005) were kept. The value of $V_{hel}$ for a galaxy with available redshift data was updated when the errors quoted in the recent bibliography were smaller than in our previous compilation. For a subset of galaxies we found that the source of the data provided in NED (NASA/IPAC Extragalactic Database) were obtained from Stocke et al. (2004) but, while the paper was providing galactocentric velocities, NED was quoting them as heliocentric. This error was reported to the NED team and was corrected in both NED and in our database. Only for 40 CIG galaxies velocity data were not found in the bibliography, hence 1010 out of 1050 CIG galaxies currently have redshift measures.

Distances were obtained from Virgo-centric velocities ($V_{vir}$) as $D = V_{vir}/H_0$ (using $H_0 = 75$ km s$^{-1}$ Mpc$^{-1}$), where $V_{vir}$ is calculated from the heliocentric velocity $V_{hel}$ and galactic coordinates following HyperLeda convention. Virgo-centric velocities were calculated as $V_{hel} = V_{lg} + 208\cos(\theta)$, where $V_{lg}$ is the radial velocity with respect to the Local Group and $\theta$ is the angular distance between the galaxy and Virgo center. In order to transform the $V_{hel}$ to $V_{vir}$ we transformed $\alpha$ and $\delta$ coordinates in Leon & Verdes-Montenegro (2003) to $l$ and $b$ values.

### 2.2. Morphologies

Sulentic et al. (2006) performed a careful revision of the morphologies for the whole CIG sample based on POSS II (Second Palomar Observatory Sky Survey; Reid et al. 1991) images. We recently revised those morphologies for all CIG galaxies with $V_{hel} > 1000$ km s$^{-1}$ and CCD images available either from SDSS or our own data ($N = 843$). For CIG galaxies with $V_{hel} < 1000$ km s$^{-1}$ ($N = 57$), morphological types were compiled from the bibliography and the mean value used. For $N = 134$ galaxies with only POSS II data available, a second revision was performed, with minor modifications to the values assigned in Sulentic et al. (2006). For the remaining galaxies for which we were unable to perform any classification, we used data found in the NED and HyperLeda database. Errors in the morphological

[1] http://www.wf4ever-project.org
[2] http://www.taverna.org.uk/
[3] http://www.myexperiment.org/packs/231.html

**Table 1.** Main properties of the CIG sample.

| CIG | $V_{hel}$ (km s$^{-1}$) | $D$ (Mpc) | $T$ (RC3) | err T | IA | $B_T$ (mag) | $A_g$ (mag) | $A_i$ (mag) | $A_K$ (mag) | $B_T^c$ (mag) | $L_B$ ($L_\odot$) | $D_{25}$ ($'$) | $d_{25}$ ($'$) | $i$ ($^o$) | Target |
|---|---|---|---|---|---|---|---|---|---|---|---|---|---|---|---|
| (1) | (2) | (3) | (4) | (5) | (6) | (7) | (8) | (9) | (10) | (11) | (12) | (13) | (14) | (15) | (16) |
| 1 | 7299.0 | 96.9 | 5.0 | 1.5 | 1 | 14.167 | 0.173 | 0.57 | 0.04 | 13.38 | 10.57 | 1.39 | 0.64 | 65.09 | 0 |
| 2 | 6983.0 | 94.7 | 6.0 | 1.5 | 0 | 15.722 | 0.255 | 0.28 | 0.03 | 15.16 | 9.840 | 0.72 | 0.50 | 46.82 | 1 |
| 3 | – | – | 4.0 | 1.5 | 0 | 16.057 | 0.246 | 0.35 | – | – | – | 0.40 | 0.24 | 55.05 | 0 |
| 4 | 2310.0 | 31.9 | 3.0 | 1.5 | 0 | 12.818 | 0.252 | 0.86 | 0.02 | 11.69 | 10.28 | 3.29 | 0.73 | 90.00 | 1 |
| 5 | 7865.0 | 105.9 | 0.0 | 1.5 | 0 | 15.602 | 0.225 | 0.13 | 0.12 | 15.13 | 9.95 | 0.73 | 0.32 | 75.47 | 1 |
| 6 | 4528.0 | 61.6 | 7.0 | 1.5 | 1 | 15.395 | 0.412 | 0.64 | 0.02 | 14.33 | 9.80 | 0.70 | 0.31 | 65.32 | 1 |
| 7 | 12 752.0 | 169.9 | 4.0 | 1.5 | 0 | 15.662 | 0.100 | 0.34 | 0.08 | 15.14 | 10.35 | 0.69 | 0.43 | 53.96 | 1 |
| 8 | 6342.0 | 85.0 | 5.0 | 1.5 | 0 | 15.624 | 0.489 | 0.73 | 0.03 | 14.37 | 10.06 | 0.75 | 0.28 | 71.68 | 0 |
| 9 | 8474.0 | 113.0 | 5.0 | 1.5 | 1 | 15.537 | 0.111 | 0.64 | 0.05 | 14.74 | 10.16 | 0.91 | 0.38 | 68.07 | 1 |
| 10 | 4613.0 | 63.6 | 5.0 | 1.5 | 0 | 15.377 | 0.366 | 0.55 | 0.03 | 14.44 | 9.78 | 1.05 | 0.50 | 63.94 | 0 |
| .. | .. | .. | .. | .. | .. | .. | .. | .. | .. | .. | .. | .. | .. | .. | |

**Notes.** The columns correspond to (1) galaxy identification according to CIG catalog; (2) heliocentric velocity; (3) distance; (4) morphological type; (5) error in the morphological type; (6) degree of optical asymmetry, (7) $B$-band magnitude from HyperLeda, (8) Galactic extinction; (9) internal extinction; (10) K-correction in the $B$-band; (11) corrected magnitude in the $B$-band; (12) logarithm of the optical luminosity in the $B$-band; (13) major axis; (14) minor axis; (15) galaxy inclination, as described in Sect. 2. In Col. (16): we flag galaxies with code 1 when the galaxy is studied in this paper, and 0 otherwise, following Sect. 3. The full table, including columns with errors and other additional information are available in electronic form at `http://amiga.iaa.es` and at the CDS.

types were estimated based on the quality of the used images as well as the angular resolution relative to the galaxy size.

There is a general shift in the morphologies with respect to Sulentic et al. (2006) toward later types by $\Delta T = 0.2$, which we interpret as being caused by the higher resolution provided by CCD images, which reveales smaller bulges. Types ($T$) were coded following RC3 (see morphological codes in Table 3). Sulentic et al. (2006) also flagged galaxies that they suspected to be interacting. We now replaced this code by a descriptive one, based also on visual inspection of the optical images, as described below. Code IA = 0 was assigned if no relevant signs of distortions are visible. Code IA = 1 corresponds to galaxies seen in the images as asymmetric, lopsided, warped or distorted, with an integral sign shape or tidal feature (tail, bridge, shell). Those galaxies were always treated separately in our analysis, to check whether they present a different behavior from those classified with code 0. Code IA = 2 was assigned if the galaxy was identified as a pair in Verley et al. (2007a) and/or in NED, or if the galaxy looks like a merger or superposition of two galaxies. These galaxies were considered not to be part of the AMIGA sample and are marked differently in the plots. The new data are presented in Table 1 and now all CIG galaxies have a morphological code.

#### 2.2.1. Apparent magnitudes

Blue optical magnitudes $B_T$ were obtained from HyperLeda (Paturel et al. 2003), not from the Catalog of Galaxies and Clusters of Galaxies (Zwicky et al. 1961–1968) as in Verdes-Montenegro et al. (2005), and the corrected $B_T^c$ was calculated as follows:

$$B_T^c = B_T - A_g - A_i - A_K, \quad (1)$$

where $A_g$ is the galactic dust extinction, $A_i$ is the internal extinction correction and $A_K$ is the K correction. $A_g$ was obtained from HyperLeda (Schlegel et al. 1998), except for CIG 447, for which only NED data were available. $A_i$ was calculated as in HyperLeda (Bottinelli et al. 1995), using their values for $\log(R_{25})$ (axis ratio of the isophote 25 mag/arcsec2 in the $B$-band for galaxies) but our own morphological types. Finally $A_K$ was obtained as defined in HyperLeda[2] ($A_K = \mathrm{ak}(T)V_{hel}/10\,000$; de Vaucouleurs et al. 1976), using our own morphologies and distances. The uncorrected and corrected magnitudes are listed in Table 1.

### 2.3. Optical luminosity

The optical luminosities were derived as

$$\log(L_B/L_\odot) = 11.95 + 2\log[D(\mathrm{Mpc})] - 0.4B_T^c, \quad (2)$$

where the solar luminosity is given in units of the solar bolometric luminosity as in Lisenfeld et al. (2007). The mean value of the difference between our new values for optical luminosities with respect to those used in Lisenfeld et al. (2007) is as small as $0.02 \pm 0.18$ mag but has the advantage of being derived from $B_T$ magnitudes compiled from HyperLeda database, which reduces the errors.

### 2.4. Optical diameter and axis ratio ($D_{25}$ and $R_{25}$)

We used the HyperLeda database to compile of the major axis $D_{25}$ (isophotal level at 25 mag/arcsec$^2$ in the $B$-band) and axis ratios $R_{25}$ ($R_{25} = D_{25}/d_{25}$, where $d_{25}$ is the minor axis, at an isophotal level of 25 mag/arcsec$^2$), as well as their errors (minor and major axis are given in Table 1).

### 2.5. Inclinations

The inclination ($i$) was determined from the value of $R_{25}$ in HyperLeda database and our revised morphological type with the following equation (Heidmann et al. 1972):

$$\sin^2(i) = \frac{1 - 10^{-2\log(R_{25})}}{1 - 10^{-2\log(R_0)}}, \quad (3)$$

where $\log(R_0) = 0.43 + 0.053 \times T$ for $T \leq 7$ and $\log(R_0) = 0.38$ for $T > 7$.

## 3. Sample selection

As a starting sample we used the catalog of 791 AMIGA galaxies selected by Verley et al. (2007b), which rejects galaxies with

[2] `http://leda.univ-lyon1.fr/leda/param/btc.html`

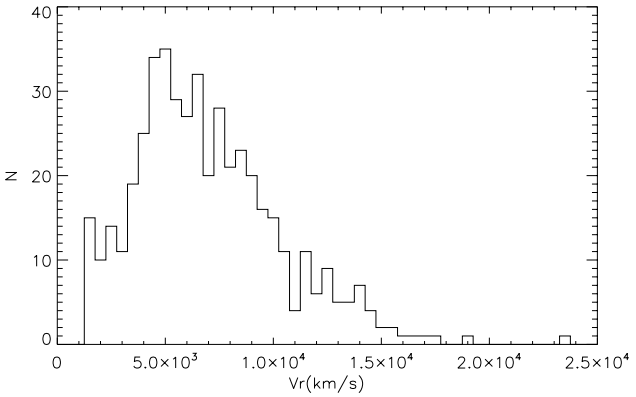


**Fig. 1.** Distribution of the heliocentric velocities of the 466 CIG galaxies used in this work.

isolation parameters $Q > -2$ and $\eta_k > 2.4$ (the tidal strength created by all neighbors, $Q$, is more than 1% of the internal binding forces; for the local number density, $\eta_k$, this translates into a value of 2.4; Athanassoula 1984) and with recession velocities $V_r < 1500$ km s$^{-1}$. These conditions imply that the evolution of all galaxies in our starting sample is dominated by their intrinsic properties (see Verley et al. 2007b, for more details). This sample is complete up to $B_T^c = 15.3$, where $B_T^c$ is the magnitude in the $B$-band from HyperLeda after corrections. The completeness limit was decided in Verdes-Montenegro et al. (2005) ($B_T^c = 15$ mag) after applying the $\langle V/Vm \rangle$ test (Schmidt 1968), and was recently updated because $B$-band magnitudes were recalculated following HyperLeda expressions in 2010 (see Sect. 2). There are 657 objects in the complete AMIGA sample that also fulfill the above isolation criteria. Photometric data used in this work come from the SDSS-III (Data Release 8, DR8 Aihara et al. 2011). The SDSS project used a 2.5 m telescope (Gunn et al. 2006) to obtain photometric information from CCD images in $u$, $g$, $r$, $i$, and $z$ passbands. A new approach for background subtraction was applied in DR8 that first models the brightest galaxies in each field so that the estimated sky background remains unaffected (Blanton et al. 2011).

From the 657 galaxies that are part of the complete AMIGA sample, we found 496 objects in the SDSS database. We found and removed 14 galaxies from the catalog that involved imprecise identifications of galaxy nuclei in the SDSS database or galaxies with a nearby bright star that adversely affected the galaxy photometry. We also removed 16 galaxies with unknown redshifts because the redshift will be needed for the following analysis. The final sample consists of 466 isolated galaxies with radial velocities between 1500 and 24 000 km s$^{-1}$. Hereafter, we refer to it as the AMIGA-SDSS sample. We present its redshift distribution in Fig. 1. This sample includes 70 galaxies with asymmetries that are suspected of being involved in interactions or that have nearby companions. These properties are represented in our sample by the degree of asymmetry IA = 1 (63) or IA = 2 (7) (see Sect. 2.2), where IA = 2 represents the most asymmetric galaxies. We did not reject these objects because we are trying to see what features a galaxy can develop in isolation, but we checked the effect of these galaxies in the median colors throughout. We focused on the two most statistically significant subsamples, which involve Sb-Sc spirals and E/S0 early-types. These involve approximately 68% and 15% of our AMIGA-SDSS sample, respectively. The Sb-Sc spirals are interpreted as a kind of "parent population" of isolated galaxies because they represent 2/3 of the total sample. The E/S0 early-types were somewhat surprising given that isolated galaxies are simply the outliers of loose groups where the early-type fraction is ∼0.4 (van der Wel et al. 2007). We found ∼0.15 in our sample, which is still large enough to be interesting. Other types are represented in such small numbers that we assume them to be simply random galaxies that happen to be unusually isolated at this time. This assumption is motivated by the standard idea that all disky galaxies with a large bulge are products of nurture. The late-type spiral population involves galaxies with small bulges (or even pseudo-bulges, Durbala et al. 2008) which, if interpreted as a secular evolution diagnostic, cannot have spent much time in richer environments.

## 4. Deriving rest-frame colors

A variety of magnitude estimates are given for each galaxy included in the SDSS catalog. We chose the model magnitudes for deriving colors in our sample because they are calculated using best-fit parameters in $r$-band that are then applied to the other bands. Model magnitudes are therefore computed through the same aperture for all bands. To compute absolute magnitudes in each band the following corrections were applied:

- A correction for Galactic dust extinction by applying the reddening corrections computed by SDSS following Schlegel et al. (1998).
- The k-correction in each band was calculated using the code `kcorrect` (Blanton & Roweis 2007), which determines the spectral energy distribution (SED) of the galaxy using SDSS photometry from a nonnegative linear combination of five templates based on the Bruzual & Charlot (2003) stellar evolution synthesis codes.
- Absolute magnitudes were calculated using the updated distances shown in Table 1.

The internal extinction correction in $B$-band was calculated by Verdes-Montenegro et al. (2005) as a function of inclination and morphological type following de Vaucouleurs et al. (1991). We used the Calzetti law (Calzetti et al. 2000) for deriving the SDSS-band internal extinctions based on the $B$-band corrections. We represented the rest-frame color $(g - r)$ versus inclination before and after the extinction corrections and found that this correction was overestimated (the slope of the linear regression changes from 0.17 to −0.21 for Sc galaxies and from 0.16 to −0.13 for Sb galaxies, after corrections). Masters et al. (2010) studied the effect of this correction on the colors through its dependency on inclination, spiral type and absolute magnitude. The best result for our $(g - r)$ versus inclination plots is obtained using a linear combination of their relations as defined in Eq. (3) in Masters et al. (2010) (the slope of the $(g - r)$ versus inclination relation after this correction is 0.025 for Sc and 0.023 for Sb galaxies), while the expressions these authors give for each morphological type (bulge-disk ratio) produce an overcorrection in all our subsamples. We also note that the dependence of the internal extinction correction on galaxy luminosity derived in Masters et al. (2010) is not reproduced by our data. If AMIGA spirals are indeed more dynamically quiescent systems, it is perhaps not surprising that corrections derived from almost certainly less quiescent samples would yield different corrections. Moreover, this preliminary result of lower extinction in AMIGA spirals can be understood as a sign of less dust because we assumed that the star formation has been lower in our isolated galaxies for all or most of their lives (Leon et al. 2008).

**Table 2.** Photometric information of the CIG–SDSS sample.

| CIG | $g$ | $A_g(g)$ | $A_K(g)$ | $M_g$ | $r$ | $A_g(r)$ | $A_K(r)$ | $M_r$ | $A_i(g-r)$ | $(g-r)$ |
|---|---|---|---|---|---|---|---|---|---|---|
| | (mag) | (mag) | (mag) | (mag) | (mag) | (mag) | (mag) | (mag) | (mag) | (mag) |
| (1) | (2) | (3) | (4) | (5) | (6) | (7) | (8) | (9) | (10) | (11) |
| 2 | 15.317 | 0.223 | 0.030 | –19.869 | 14.677 | 0.162 | 0.028 | –20.446 | 0.000 | 0.577 |
| 4 | 13.442 | 0.220 | 0.013 | –19.325 | 12.611 | 0.160 | 0.011 | –20.094 | 0.092 | 0.677 |
| 5 | 15.464 | 0.197 | 0.072 | –19.986 | 14.658 | 0.143 | 0.028 | –20.694 | 0.000 | 0.708 |
| 6 | 14.841 | 0.361 | 0.005 | –19.507 | 14.338 | 0.262 | 0.012 | –19.917 | 0.000 | 0.411 |
| 7 | 14.924 | 0.088 | 0.101 | –21.507 | 14.120 | 0.064 | 0.063 | –22.248 | 0.029 | 0.712 |
| 9 | 15.318 | 0.098 | 0.056 | –20.162 | 14.612 | 0.071 | 0.042 | –20.828 | 0.053 | 0.613 |
| 12 | 15.532 | 0.263 | 0.024 | –19.127 | 14.849 | 0.191 | 0.025 | –19.740 | 0.068 | 0.545 |
| 14 | 14.198 | 0.574 | 0.044 | –20.743 | 13.212 | 0.416 | 0.015 | –21.542 | 0.000 | 0.798 |
| 15 | 16.019 | 0.131 | 0.075 | –20.247 | 15.177 | 0.095 | 0.076 | –21.054 | 0.053 | 0.754 |
| 17 | 15.439 | 0.110 | 0.065 | –20.854 | 14.773 | 0.080 | 0.067 | –21.492 | 0.018 | 0.620 |
| .. | .. | .. | .. | .. | .. | .. | .. | .. | .. | .. |

**Notes.** The columns correspond to (1): galaxy identification according to CIG catalog; (2): $g$-band model magnitude from SDSS–DR8; (3): Galactic extinction in the $g$-band from SDSS–DR8; (4): $k$-correction in the $g$-band; (5): absolute magnitude in the $g$-band; (6): $r$-band model magnitude from SDSS–DR8; (7): Galactic extinction in the $r$-band from SDSS–DR8; (8): $k$-correction in the $r$-band; (9): absolute magnitude in the $r$-band; (10): internal extinction correction in the $(g-r)$ color; (11): corrected $(g-r)$ rest-frame color. The full table is available in electronic form at http://amiga.iaa.es and at the CDS.

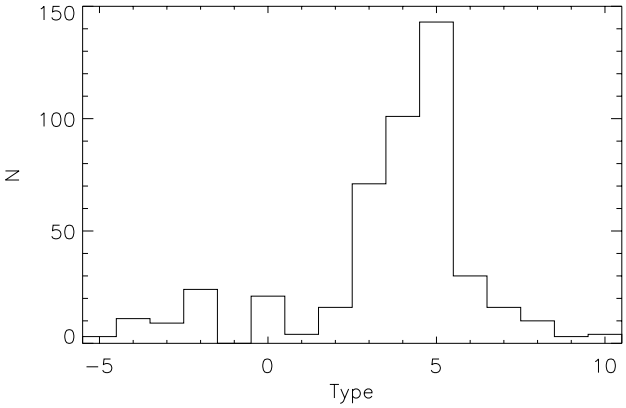


**Fig. 2.** Distribution of Hubble types in the AMIGA-SDSS sample.

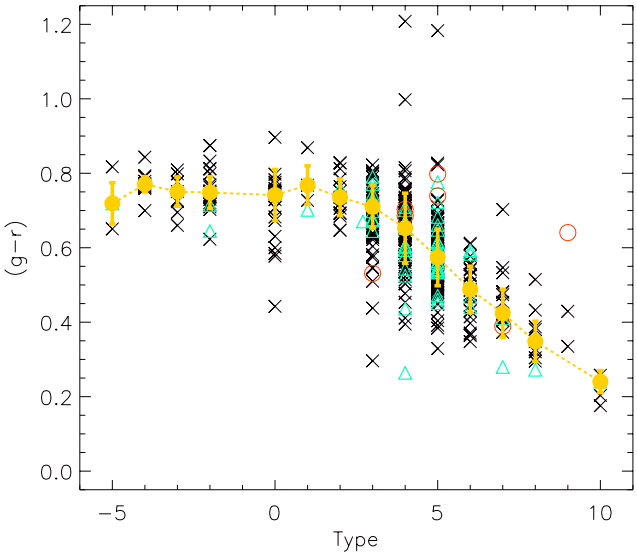


**Fig. 3.** Distribution of the rest-frame $(g-r)$ color as a function of Hubble type. The yellow points are the median values of each morphological type. The blue triangles are objects with asymmetry index IA = 1 while the red open points represent the most asymmetric objects (IA = 2) in our sample. The error bars represent the median absolute deviation.

Finally, we applied the correction of Masters et al. (2010), based on their Eq. (3), to our Sa-Sc galaxies. We did not correct morphological types earlier than 0 (E/S0) and later than 6 (Scd/Sd/Irr) because their numbers are small and their $(g-r)$ vs. inclination plots do not show any clear trend of color vs. $i$ (the slope of the fits is ∼0). Photometric data as well as colors for the AMIGA–SDSS sample are presented in Table 2.

## 5. $(g-r)$ color as a function of morphological type

In Fig. 2 we presented the number of galaxies in the AMIGA-SDSS sample for each morphological subtype, and Fig. 3 shows the distribution of SDSS $(g-r)$ colors for the AMIGA sample as a function of the morphological subtype. We calculated the median values and not the mean values, because they are less sensitive to outliers produced by an error in the color for one object or misclassification. We used the median absolute deviation as a scatter measure since it represents a robust estimator of dispersion for median values. Not surprisingly, the reddest median values of $(g-r)$ are found for the first four bins, which represent early-type galaxies, although median $(g-r)$ values remain essentially constant out to $T = 3$ (Sb). Beginning with type Sb we see a decrease in median $(g-r)$ as expected if this sequence reflects a uniformly decreasing contribution from an old stellar population (Strateva et al. 2001; Blanton et al. 2003).

Surprisingly, the color distributions for our late-type spiral Sb-Sc population show some galaxies with colors even redder than the E/S0 subsample. Either AMIGA early-type galaxies are extraordinarily blue or these spirals have anomalous colors. Careful examination of these objects using the SDSS navigation tool shows that colors of the reddest Sb-Sc galaxies are unreliable and/or that the assigned galaxy types are incorrect. For our Sc subsample (which is perhaps the easiest to classify) we find $n = 10$ galaxies with $(g-r) > 0.7$ (typical colors of early-types). In eight cases there is a problem with the color: 1) five are affected by a star projected onto or very close to the galaxy (CIG 261, 304, 649, 716, 1010); 2) two (CIG 349, 946) belong to the seven galaxies previously identified with a high degree of asymmetry (IA = 2); 3) one (CIG 988) is highly inclined and the extinction correction (Masters et al. 2010) could be maximally affected by the uncertainty of the adopted inclination. Of the remaining two red Sc spirals, one (CIG 709) shows almost the highest recession velocity in our sample ($V > 14\,000$ km s$^{-1}$).

At this distance the number of resolution elements in the galaxy images approaches that of POSS II. For CIG 709, the image of SDSS shows a close object with unknown redshift, which could be a minor companion causing some kind of asymmetry in the optical bands. Finally, CIG 807 may well be an Sc spiral but the blue disk is not resolved. The point of this exercise is to show that one can identify remarkably pure isolated (local) spiral subsamples but only if the above mentioned pitfalls are taken into account. If these effects are not taken into account, the average properties of the isolated subsamples can be blurred beyond statistical utility.

The Sbc and Sb spirals show similar effects among the reddest galaxies, which only detailed surface photometry could correct. Naturally, similar problems can afflict the bluest galaxies in each spiral subtype. Colors for 2/4 of the bluest Sc spirals ($(g-r) < 0.4$) are also likely affected by their nearby bright stars. These effects can be a source of serious scatter in color distributions for any galaxy sample and illustrate the caution needed in using SDSS colors. On the other hand, while the objects with IA = 2 are outside the normal trend of the median values, the color of the AMIGA galaxies with asymmetry index IA = 1 agrees with the color of symmetric galaxies (IA = 0). In the following analysis, objects with IA = 2 were removed but not objects with spurious colors, because these also exist in the samples that we used as comparison. Nevertheless, we included their effects through the error measures.

We expected to find a lower color dispersion for spiral subtypes in the AMIGA sample because these galaxies are minimally affected by environmental effects, which apparently induce a higher color dispersion. This has been known since the first statistical study of colors for galaxies in interacting pairs and multiplets (i.e. they evolve more passively, cf. Larson & Tinsley 1978). One of the goals of the AMIGA project is to provide a sample that could better characterize intrinsic galaxy properties and their dispersions.

What is the main source of color dispersion for spiral subtypes if we have achieved our goal of minimizing effects of environmental nurture from our sample? Spirals contain a red bulge (redness depending on the nature of the bulge) and a blue disk, which makes their global $(g-r)$ color sensitive to the aperture used in estimating the $g$ and $r$ magnitudes. We checked the $(g-r)$ color versus absolute magnitude relation for Sc galaxies in three separate redshift ranges. The results are presented in Fig. 3. We find a tendency for galaxies of fixed absolute magnitude to be $(g-r) \sim 0.08$ redder at lower recession velocities, implying that the color measures in our sample could be increasingly affected by bulge light at lower recession velocities. This is a minor but systematic effect. However, an aperture effect will also underestimate the absolute magnitude of the galaxy, making it more difficult to estimate the amplitude of the color bias.

Figure 4 shows that the major source of color dispersion in Fig. 3 is connected with the color-luminosity trend. Sb-Sc color distributions show Gaussian distributions for each subtype with FWHM = 0.15–0.2, spanning almost 2 dex in luminosity ($M_r = -19$ to $-22.5$). The effect is strongest for Sc spirals in our sample where the color-luminosity trend appears to be steeper (Sc spirals with $M_r = -22.5$ are ~0.25 mag redder than Sc spirals with $M_r = -19$). Figure 4 also shows the $(g-r)$ vs. $M_r$ density diagram obtained from the Nair & Abraham (2010) sample covering the range $0.01 < z < 0.05$ (SDSS DR8). This sample was accumulated without morphology or environmental selections, therefore we see the bimodality previously found for SDSS data (Strateva et al. 2001; Blanton et al. 2003). The distribution of our Sc subsample evidently follows the blue sequence

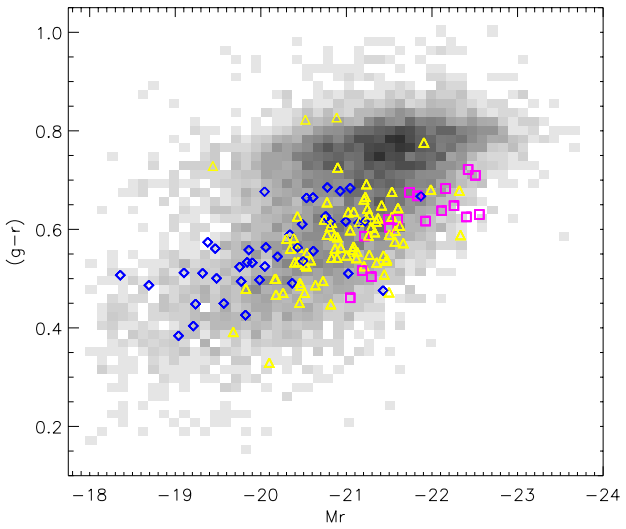


**Fig. 4.** $(g-r)$ color–magnitude diagram for the Sc galaxies in the AMIGA sample. The blue diamonds are objects at $z < 0.02$, the yellow triangles are galaxies at redshift $0.02 < z < 0.04$, and the pink squares are objects at $z > 0.04$. The gray scale represents the density diagram obtained from the Nair & Abraham (2010) sample at $0.01 < z < 0.05$, using the data of DR8.

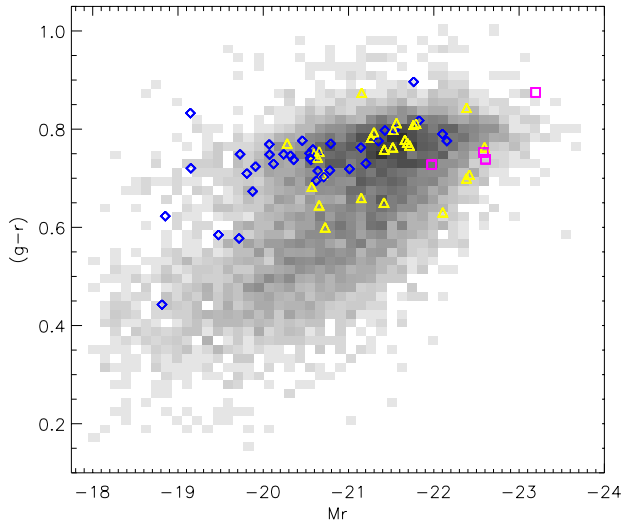


**Fig. 5.** Same as Fig. 4 but for the E/S0 galaxies in the AMIGA sample.

with the recession velocity vs. color bias. The same bias in the color as a function of redshift was found by using the sample of Nair & Abraham (2010). Moreover, for a given luminosity and morphological type (Sc), the petrosian radius $R_{90}$ given in the SDSS database for the Nair & Abraham (2010) sample decreases with lower redshifts. The main trend of our data in the figure (and hence the source of the color dispersion) clearly involves the color-luminosity correlation. The overlap (i.e. green valley) instead of being a class of galaxies with intermediate colors, may be entirely due to spirals with spurious red colors caused by the effects discussed above. The $(g-r)$ vs. $M_r$ diagram for a vetted sample of isolated galaxies shows a much clearer dichotomy than other samples. There is no evidence for an astrophysically significant green valley, but we need more reliable colors to confirm this result.

Figure 5 shows an equivalent diagram for the early-type (E/S0) part of the AMIGA sample. Despite their isolation, they fall in the red sequence defined by early-types in richer

**Table 3.** Median $(g - r)$ colors as a function of morphological type.

| Type | $T$ | AMIGA | NAIR | EFIGI | CPG (WID) | CPG (CLO) |
|---|---|---|---|---|---|---|
| E | –5 | 0.72 ± 0.06 | 0.78 ± 0.03 | 0.78 ± 0.03 | 0.79 ± 0.03 | 0.76 ± 0.03 |
| E | –4 | 0.77 ± 0.02 | – | 0.78 ± 0.02 | 0.80 ± 0.08 | 0.79 ± 0.04 |
| E/S0 | –3 | 0.75 ± 0.04 | 0.76 ± 0.05 | 0.77 ± 0.04 | 0.79 ± 0.06 | 0.77 ± 0.07 |
| S0 | –2 | 0.75 ± 0.04 | 0.76 ± 0.04 | 0.76 ± 0.04 | 0.78 ± 0.06 | 0.77 ± 0.06 |
| S0 | –1 | – | – | 0.78 ± 0.06 | 0.72 ± 0.05 | 0.73 ± 0.09 |
| S0/a | 0 | 0.74 ± 0.07 | – | 0.76 ± 0.07 | 0.77 ± 0.05 | 0.78 ± 0.04 |
| Sa | 1 | 0.77 ± 0.05 | 0.71 ± 0.06 | 0.73 ± 0.05 | 0.72 ± 0.11 | 0.71 ± 0.09 |
| Sab | 2 | 0.74 ± 0.05 | 0.69 ± 0.07 | 0.72 ± 0.07 | 0.71 ± 0.10 | 0.67 ± 0.15 |
| Sb | 3 | 0.71 ± 0.06 | 0.67 ± 0.08 | 0.71 ± 0.08 | 0.71 ± 0.13 | 0.69 ± 0.12 |
| Sbc | 4 | 0.65 ± 0.09 | 0.61 ± 0.08 | 0.66 ± 0.07 | 0.63 ± 0.12 | 0.59 ± 0.14 |
| Sc | 5 | 0.57 ± 0.08 | 0.56 ± 0.08 | 0.62 ± 0.09 | 0.69 ± 0.12 | 0.51 ± 0.15 |
| Scd | 6 | 0.49 ± 0.06 | 0.46 ± 0.07 | 0.58 ± 0.09 | 0.55 ± 0.11 | 0.51 ± 0.17 |
| Sd | 7 | 0.42 ± 0.06 | 0.42 ± 0.06 | 0.47 ± 0.08 | 0.34 ± 0.17 | 0.43 ± 0.10 |
| Sdm | 8 | 0.35 ± 0.05 | 0.41 ± 0.07 | 0.44 ± 0.12 | 0.48 ± 0.07 | 0.30 ± 0.12 |
| Sm | 9 | – | 0.36 ± 0.09 | 0.40 ± 0.16 | – | 0.56 ± 0.13 |
| Im | 10 | 0.24 ± 0.03 | 0.33 ± 0.10 | 0.29 ± 0.09 | – | 0.29 ± 0.12 |

environments (e.g. Nair & Abraham 2010). They do not provide evidence for a green valley. Our early-type subsample shows no color trend with recession velocity. We notice only a slight trend between color and luminosity (galaxies with $M_r = -22.5$ are ∼0.1 mag redder than galaxies with $M_r = -19$). For early-types the FWHM of the Gaussian fit to the color distribution is ∼0.14 (similar to Sb galaxies color distribution). The bluest galaxies might be misclassified as E/S0 although photometric study of a few of them (Marcum et al. 2004) suggests that they may not be spirals. In addition, three (CIG 264, 981, and 1025) that showed HI emission were revised to check for the presence of peculiarities in the morphologies, such as dust lanes, optical shells, blue cores, or star formation. All of them were confirmed as early-type galaxies (Espada 2006).

## 6. Color dependence on environment

Some studies have shown that galaxies of a fixed morphology in higher density environments are redder (Ball et al. 2008; Skibba et al. 2009) and the reason might be that dense environments suppress star formation (Balogh et al. 1998). On the other hand, isolated galaxies are likely to show passive star formation, which leads one to expect spirals in richer environments (e.g. pairs, even the isolated pairs usually included in field galaxies samples) to show a more active star formation and hence bluer colors (Patton et al. 2011). Larson & Tinsley (1978) found a higher color dispersion in an extreme nurture sample, whose evolution is completely dominated by external effects. The key word here is dispersion: colors of galaxies in pairs and groups are not systematically bluer, but they show a higher color dispersion. The AMIGA sample of galaxies involves some of the most isolated objects in the local Universe that are minimally affected by external processes, at least during the past few Gyr. We therefore expect that AMIGA galaxies of a given morphological type will show minimal color dispersion and the above results support that expectation.

Table 3 provides a quantitative comparison of $(g - r)$ median colors in our sample and in samples involving denser environments. We used three catalogs for this comparison: 1) Nair & Abraham (2010), which includes a detailed visual classifications for 14,034 galaxies in the SDSS DR4. We selected only objects with morphological classification available and redshift $0.01 < z < 0.05$ (8976) to better match our AMIGA-SDSS sample (98%); 2) the EFIGI catalog (Baillard et al. 2011), which provides detailed morphological information for a sample of 4458 PGC galaxies, also using SDSS DR4. Both samples include galaxies in a wide range of environments. 3) We also compared our data with the catalog of isolated pairs of galaxies (CPG, Karachentsev 1972), composed of 1206 objects. It was visually compiled, like CIG, using POSS II and applying an isolation criterion.

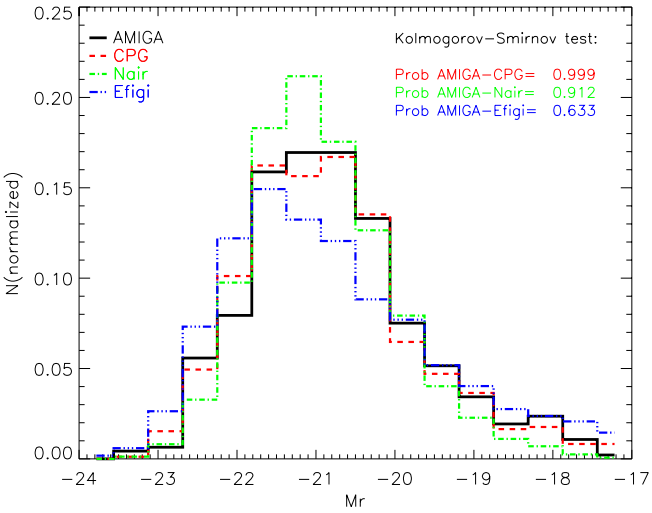


**Fig. 6.** Distribution of absolute magnitudes in the $r$-band for the whole AMIGA-SDSS sample, and for the Nair & Abraham (2010), Efigi, and CPG samples described in the text.

We used SDSS DR8 photometric data for all three samples and derived rest-frame colors in the same way as for our sample. For the CPG sample, there are 916 galaxies with SDSS photometry. We calculated the projected distance between galaxies in each pair using redshifts taken from HyperLeda. Following Xu & Sulentic (1991), we separated this sample into close-interacting (CLO – galaxies with separation SEP < 2 Mpc) and wide (WID) pairs (SEP > 2 Mpc). We checked the distribution of redshift and absolute magnitudes in the r-band for each sample and found good agreement with the whole AMIGA-SDSS sample. In the cases of EFIGI and CPG catalogs, we removed the objects with recession velocities lower than 1500 km s$^{-1}$ as we did for our AMIGA sample, because the determination of the isolation parameters (Verley et al. 2007b). We also removed objects fainter than $M_r > -17$ since we do not have counterparts in the AMIGA-SDSS sample. The final samples

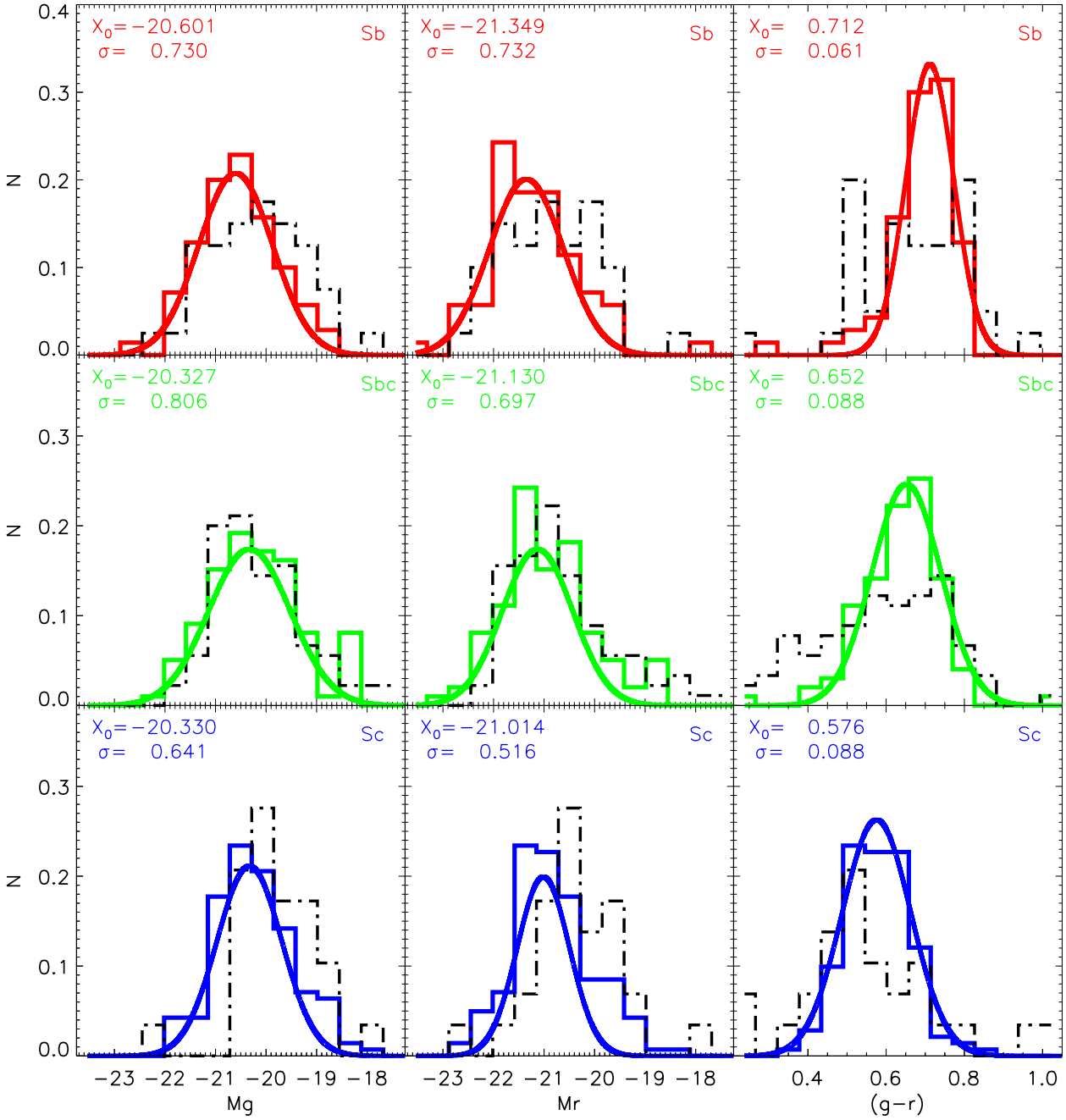


**Fig. 7.** Distribution of absolute magnitudes in the *g*-band (*left*), *r*-band (*center*) and $(g - r)$ color (*right*) for all Sb (*top*), Sbc (*middle*) and Sc (*bottom*) galaxies. The solid lines represent the AMIGA-SDSS sample and the dashed lines are the distribution of the CPG close pairs.

of comparison have 8879 (Nair), 3294 (EFIGI), and 839 (CPG) galaxies. In Fig. 6 we present the absolute magnitude distribution in the *r*-band for each sample, as well as the probability given by the Kolmogorov-Smirnov two-sample test that these distributions are indistinguishable from the AMIGA-SDSS one. This probability is higher than 90% for the CPG and Nair samples, while the lowest value is found for the EFIGI sample (63%).

We found good agreement for the colors of early-type galaxies in all samples. However, throughout (from $T = -5$ to $T = 0$), the median values for the AMIGA sample are a slightly bluer (but within the errors) than the other samples. Because the color-luminosity relation has a trend (brighter galaxies are redder), this bluer color could be presumably arise because the E/S0 population of AMIGA is fainter than any other sample (Sulentic et al. 2006). The median values of colors for the Nair & Abraham (2010) and close pair samples for the (Sb-Sc) spirals are consistent but slightly bluer than our sample. For the comparison with Nair & Abraham (2010), the differences in color may be produced by the different morphological classifications used in both samples. We find their morphologies to be earlier than ours, with a mean deviation of ∼1.5 for each Hubble type. To test this possibility, we selected a subsample composed of the 142 common objects between AMIGA and the Nair & Abraham (2010) sample, and calculated the median values of $(g - r)$ obtained using each morphological classification. We found that the difference between both median colors in the common sample was consistent with that found using the full samples.

Nevertheless, the differences in color of close pairs seem to be more robust because the colors of wide pairs are as red as

the colors of isolated galaxies. The scatter is also larger for the close pairs, in agreement with Larson & Tinsley (1978). In Fig. 7 we present the distribution of absolute magnitudes in $r$ and $g$-bands as well as $(g-r)$ color for three morphological types (Sb, Sbc and Sc) of the AMIGA-SDSS sample. We also represented the same distributions for the close pairs of the CPG sample. While the color distribution of each morphological type has a Gaussian distribution for our sample, the color histogram for the CPG sample follows a non-Gaussian distribution. The loss of Gaussianity in the distribution of color can be interpreted as an effect of the environmental nurture that occurs in a sample of pairs.

We have also investigated the change in the median colors when we rejected objects with asymmetries (IA = 1), and the differences are negligible.

## 7. Conclusions

We have taken a first look at the colors of isolated galaxies using SDSS $g$- and $r$-magnitudes. A first look is also inevitably an introduction into the pitfalls of using the SDSS automated measures of magnitudes. We found that the color distributions of morphological subtypes can be well described as Gaussian distributions with FWHM $(g-r) = 0.1$–$0.2$. This is expected for samples where effects of environmental nurture have been minimized, and is supported by the fact that this Gaussianity was not observed in the sample of galaxy pairs. Most of the color dispersion of spiral subtypes is caused by a color-luminosity correlation, with more massive spirals showing redder colors. Indeed, most of the Sb spirals in our sample are concentrated in the upper region of the blue cloud, below the red sequence. We saw little evidence for a green valley in our sample, with most spirals redder than $(g-r) = 0.7$ having spurious colors (~80%). We found a preliminary difference in the color of the isolated and paired spiral galaxies. The median value of $(g-r)$ seems to be bluer when interactions are included. Nevertheless, no difference was found in the $(g-r)$ color of early-type galaxies, which suggests that the bluer color of spirals in pairs is presumably due to interaction-enhanced star formation. Our sample of isolated galaxies gives a median absolute deviation in color that is lower than that in pairs of galaxies, where a more active star formation and, perhaps, a higher dust diffusion caused by the interaction, are also sources of color dispersion. The mean colors and dispersions for isolated galaxy subtypes (especially E/S0 and Sb-Sc) are likely the best nurture–free measures obtained so far.

*Acknowledgements.* This work has been supported by Grant AYA2008-06181-C02 co-financed by MICINN and FEDER funds, and the Junta de Andaluca (Spain) grants P08-FQM-4205 and TIC-114. We are grateful to the AMIGA team for the great work they have done on improving the sample and to the anonymous referee for useful comments. Wf4Ever is funded by the Seventh Framework Programme of the European Commission (Digital Libraries and Digital Preservation area ICT-2009.4.1 project reference 270192). We are grateful to all our collaborators in this project. We thank the SDSS group for making their catalogues and data publicly available. Funding for SDSS-III has been provided by the Alfred P. Sloan Foundation, the Participating Institutions, the National Science Foundation, and the U.S. Department of Energy. The SDSS-III web site is http://www.sdss3.org/. SDSS-III is managed by the Astrophysical Research Consortium for the Participating Institutions of the SDSS-III Collaboration including the University of Arizona, the Brazilian Participation Group, Brookhaven National Laboratory, University of Cambridge, University of Florida, the French Participation Group, the German Participation Group, the Instituto de Astrofisica de Canarias, the Michigan State/Notre Dame/JINA Participation Group, Johns Hopkins University, Lawrence Berkeley National Laboratory, Max Planck Institute for Astrophysics, New Mexico State University, New York University, Ohio State University, Pennsylvania State University, University of Portsmouth, Princeton University, the Spanish Participation Group, University of Tokyo, University of Utah, Vanderbilt University, University of Virginia, University of Washington, and Yale University. We thank the SAO/NASA Astrophysics Data System (ADS) that is always so useful.

## References

Aihara, H., Allende Prieto, C., An, D., et al. 2011, ApJS, 193, 29
Athanassoula, E. 1984, Phys. Rep., 114, 321
Baillard, A., Bertin, E., de Lapparent, V., et al. 2011, A&A, 532, A74
Baldry, I. K., Glazebrook, K., Brinkmann, J., et al. 2004, ApJ, 600, 681
Baldry, I. K., Balogh, M. L., Bower, R. G., et al. 2006, MNRAS, 373, 469
Balogh, M. L., Schade, D., Morris, S. L., et al. 1998, ApJ, 504, L75
Ball, N. M., Loveday, J., & Brunner, R. J. 2008, MNRAS, 383, 907
Blanton, M. R., & Roweis, S. 2007, AJ, 133, 734
Blanton, M. R., Hogg, D. W., Bahcall, N. A., et al. 2003, ApJ, 594, 186
Blanton, M. R., Kazin, E., Muna, D., Weaver, B. A., & Price-Whelan, A. 2011, AJ, 142, 31
Bottinelli, L., Gouguenheim, L., Paturel, G., & Teerikorpi, P. 1995, A&A, 296, 64
Bruzual, G., & Charlot, S. 2003, MNRAS, 344, 1000
Calzetti, D., Armus, L., Bohlin, R. C., et al. 2000, ApJ, 533, 682
Capak, P., Abraham, R. G., Ellis, R. S., et al. 2007, ApJS, 172, 284
de Vaucouleurs, G., de Vaucouleurs, A., & Corwin, H. G., Jr. 1976, in Second reference catalogue of bright galaxies (Austin: University of Texas Press), 6, 396
de Vaucouleurs, G., de Vaucouleurs, A., Corwin, H. G., Jr., et al. 1991, Vol. 1–3, XII, 2069, (Berlin Heidelberg New York: Springer-Verlag)
Dressler, A. 1980, ApJ, 236, 351
Durbala, A., Sulentic, J. W., Buta, R., & Verdes-Montenegro, L. 2008, MNRAS, 390, 881
Espada, D. 2006, Ph.D. Thesis
Espada, D., Verdes-Montenegro, L., Huchtmeier, W. K., et al. 2011, A&A, 532, A117
Fouque, P., & Paturel, G. 1985, A&A, 150, 192
Gunn, J. E., Siegmund, W. A., Mannery, E. J., et al. 2006, AJ, 131, 2332
Heidmann, J., Heidmann, N., & de Vaucouleurs, G. 1972, MmRAS, 75, 105
Hogg, D. W., Blanton, M. R., Eisenstein, D. J., et al. 2003, ApJ, 585, L5
Hogg, D. W., Blanton, M. R., Brinchmann, J., et al. 2004, ApJ, 601, L29
Iovino, A. 2002, AJ, 124, 2471
Karachentsev, I. D. 1972, Soobshcheniya Spetsial'noj Astrofizicheskoj Observatorii, 7, 1
Karachentseva, V. E. 1973, Astrofizicheskie Issledovaniia Izvestiya Spetsial'noj Astrofizicheskoj Observatorii, 8, 3
Larson, R. B., & Tinsley, B. M. 1978, ApJ, 219, 46
Leon, S., & Verdes-Montenegro, L. 2003, A&A, 411, 391
Leon, S., Verdes-Montenegro, L., Sabater, J., et al. 2008, A&A, 485, 475
Lewis, I., Balogh, M., De Propris, R., et al. 2002, MNRAS, 334, 673
Lisenfeld, U., Verdes-Montenegro, L., Sulentic, J., et al. 2007, A&A, 462, 507
Lisenfeld, U., Espada, D., Verdes-Montenegro, L., et al. 2011, A&A, 534, A102
Marcum, P. M., Aars, C. E., & Fanelli, M. N. 2004, AJ, 127, 3213
Masters, K. L., Nichol, R., Bamford, S., et al. 2010, MNRAS, 404, 792
Nair, P. B., & Abraham, R. G. 2010, ApJS, 186, 427
Patton, D. R., Ellison, S. L., Simard, L., McConnachie, A. W., & Mendel, J. T. 2011, MNRAS, 412, 591
Paturel, G., Fouque, P., Bottinelli, L., & Gouguenheim, L. 1989, A&AS, 80, 299
Paturel, G., Theureau, G., Bottinelli, L., et al. 2003, A&A, 412, 57
Reid, I. N., Brewer, C., Brucato, R. J., et al. 1991, PASP, 103, 661
Sabater, J., Leon, S., Verdes-Montenegro, L., et al. 2008, A&A, 486, 73
Sabater, J., Verdes-Montenegro, L., Leon, S., et al. 2012, A&A, submitted
Schlegel, D. J., Finkbeiner, D. P., & Davis, M. 1998, ApJ, 500, 525
Skibba, R. A., Bamford, S. P., Nichol, R. C., et al. 2009, MNRAS, 399, 966
Schmidt, M. 1968, ApJ, 151, 393
Stocke, J. T., Keeney, B. A., Lewis, A. D., Epps, H. W., & Schild, R. E. 2004, AJ, 127, 1336
Sulentic, J. 2010, Galaxies in Isolation: Exploring Nature Versus Nurture, 421, 3
Sulentic, J. W., Verdes-Montenegro, L., Bergond, G., et al. 2006, A&A, 449, 937
Strateva, I., Ivezić, Ž., Knapp, G. R., et al. 2001, AJ, 122, 1861
van der Wel, A., Holden, B. P., Franx, M., et al. 2007, ApJ, 670, 206
van der Wel, A., Bell, E. F., Holden, B. P., Skibba, R. A., & Rix, H.-W. 2010, ApJ, 714, 1779
Verdes-Montenegro, L., Sulentic, J., Lisenfeld, U., et al. 2005, A&A, 436, 443
Verley, S., Odewahn, S. C., Verdes-Montenegro, L., et al. 2007a, A&A, 470, 505
Verley, S., Leon, S., Verdes-Montenegro, L., et al. 2007b, A&A, 472, 121
Xu, C., & Sulentic, J. W. 1991, ApJ, 374, 407
York, D. G., Adelman, J., Anderson, J. E., Jr., et al. 2000, AJ, 120, 1579
Zwicky, F., Herzog, E., Karpowicz, M., Kowal, C., & Wild, P. 1961–1968, Catalogue of Galaxies and of Cluster of Galaxies, Pasadena, California Institute of Technology, CGCG